Intrusion of nonwetting liquid in paper

J. Hyväluoma, T. Turpeinen, P. Raiskinmäki, A. Jäsberg, A. Koponen, M. Kataja, and J. Timonen
Department of Physics, University of Jyväskylä, FI-40014 Jyväskylä, Finland

S. Ramaswamy
Department of Wood and Paper Science, University of Minnesota, St. Paul, Minnesota 55108, USA
(Received 12 June 2006; revised manuscript received 28 December 2006; published 1 March 2007)

The saturation curve of a sample of paper board was measured with mercury-intrusion porosimetry, and the three-dimensional structure of its pore space was determined by x-ray tomographic imaging. *Ab initio* numerical simulation of intrusion on the tomographic reconstruction, based on the lattice-Boltzmann method, was in excellent agreement with the measured saturation curve. A numerical invasion-percolation simulation in the same tomographic reconstruction showed good agreement with the lattice-Boltzmann simulation. The access function of the sample, determined from the saturation curve and the pore-throat distribution determined from the tomographic reconstruction, indicated that the ink-bottle effect is significant in paperlike materials.

DOI: 10.1103/PhysRevE.75.036301 PACS number(s): 47.56.+r, 81.05.Rm

Mercury-intrusion porosimetry (MIP) is a widely used technique for pore-size characterization [1,2]. MIP measurements are fast and easy to perform, and the method is applicable to pore sizes varying over several orders of magnitude. For most materials of interest mercury is a nonwetting liquid; i.e., an external pressure is needed to make mercury intrude the pores of the sample. By increasing the pressure of the mercury in which the sample is immersed, increasingly smaller pores of it are filled and the volume of the intruded mercury is measured as a function of pressure.

In the everyday use of this method, interpretation of the measured volume is still mostly based on the assumption that pores are nonintersecting cylindrical capillaries with circular cross section and that all pores are equally accessible—i.e., connected to sample surface directly or through larger pores. By considering a liquid column in one such pore and balancing the forces resulting from the surface tension and external pressure, one obtains the Washburn equation [3]

$$\Delta p = \frac{2\gamma \cos\theta}{r}, \tag{1}$$

where Δp is the pressure difference across the meniscus (capillary pressure), γ the surface tension and θ the contact angle of the liquid, and r the radius of the pore. This equation provides a relationship between the applied pressure and the pore size intruded, and is commonly used to convert the result of measurement to a cumulative porosity as a function of pore size.

The assumptions thus made on the pore structure are not, however, valid for most real materials. The pore space can hardly be expected to resemble a system of nonintersecting capillaries. A fraction of the pores will also be connected to the sample surface only through smaller pores and will not be filled before these. The volume of small pores is thus overestimated by the equal-access assumption. This "ink-bottle effect" has already been described by Ritter and Drake [4] and Meyer [5]. Direct evidence of the size of this effect is, however, very limited (see Ref. [6]). This effect leads to the introduction within percolation theory of the access function, which, for a given external pressure, is the fraction of the allowed pore space actually accessible to the invading liquid [2]. This access function can be solved analytically for the Bethe lattice [7], but it has been difficult to determine it for real materials.

It has also been proposed [2,8,9] that the pressure dependence of the intruded volume measures a kind of pore-throat distribution rather than the pore-size distribution, which is plausible although there is hardly any direct evidence available. This assumption is also made in the invasion-percolation (IP) approach to intrusion [2]. The intrusion-extrusion hysteresis evident in most cases in MIP can be explained by IP. The extrusion phase actually probes the pore-size distribution, but due to a nontrivial access function, the extrusion curve deviates from the intrusion curve with a residual saturation at vanishing external pressure. There are also views, however, by which the difference in the advancing and retreating contact angles in the intrusion and extrusion phases, respectively, can explain the "apparent" hysteresis [1].

Difficulties with the interpretation of MIP data for some common materials have even led to rather pessimistic views of its applicability [10]. Recently attempts have been made to compare MIP results with those of image analysis [11,12], while *ab initio* computer simulations have not been employed to analyze MIP. One has mostly analyzed filling of pore space based on the Washburn equation [13,14]).

In this article we report the results of a detailed study of MIP on paper board [15], in which experimental MIP data, and also image analysis, *ab initio* fluid-flow simulations and a numerical model of IP based on a high-resolution tomographic reconstruction of the same paper board are considered. The fluid-flow simulation is based on the lattice-Boltzmann (LB) method, and it is used to describe the intrusion in the sample of a nonwetting liquid under external pressure.

In the LB method fluid is modeled by fictitious fluid particles and a discretized (space, time, and velocity are all discrete) kinetic equation is solved on a regular grid for their velocity-distribution functions. The LB algorithm consists of two phases: advection and collision. In the advection phase

distribution functions are moved to neighboring lattice nodes. Particle collisions are modeled such that distributions are relaxed towards their local equilibria. The relaxation-time parameter can be exploited in adjusting the viscosity of the fluid. Macroscopic quantities such as fluid density and velocity are obtained as velocity moments of the distributions in analogy with continuum kinetic theory, and pressure is obtained from an equation of state. Through a Chapman-Enskog analysis, one can show that the macroscopic quantities obey the Navier-Stokes equation [16,17].

In order to model a fluid with multiple phases, we use here the multiphase model by Shan and Chen [18] based on interparticle potentials. Auxiliary forces are added between neighboring fluid nodes and between fluid and wall nodes. The strengths of these forces can be adjusted so as to change the surface tension and the contact angle, respectively. In this model, an automatic separation into liquid and gas phases occurs. There is no need to track the positions of the liquid-gas interfaces as the contact-line dynamics automatically follows from the auxiliary microscopic interactions. Further details and benchmarks to the numerical methods used here can be found in Ref. [19]. LB simulations of two-phase and two-component fluid flow in porous media have been reported by several authors; see, e.g., Refs. [20–25].

In contrast with previous simulation studies on MIP [13,14], our approach is to solve the actual flow equations in the pore structure given by x-ray-computed microtomography (μCT) and to thereby mimic the intrusion process in a realistic manner. In μCT a large set of images is obtained by passing radiation through the sample in different directions. The projections thus produced can be combined so as to reconstruct the interior structure of the sample. Here the μCT imaging of the sample (paper board with a basis weight of 300 $\mathrm{g/m^{-2}}$) was done with a SkyScan 1072 system. Simulations were performed in a tomographic reconstruction of this sample of size 0.46 mm$\times$0.46 mm$\times$0.2 mm, with a voxel size of about $(2\ \mu\mathrm{m})^3$. In the transverse direction this reconstruction contains the whole thickness of the sample.

In the LB simulation, the standard MIP measurement carried out for the same paper board was realized by adding liquid on top of two opposite surfaces of the sample. The pressure of the liquid was then gradually increased, and the amount of liquid intruding the sample was recorded for each pressure increment.

According to the classification by Lenormand *et al.* [26], immiscible displacement in a porous medium can be characterized by two dimensionless variables: capillary number $\mathrm{Ca}=q\mu_n/\gamma$ and viscosity ratio $M=\mu_n/\mu_w$. Here, q is the mean flow velocity and μ_w and μ_n are the viscosities of the wetting and nonwetting fluids, respectively. In the present case we had $\log_{10}(M)\sim 1$ and $\log_{10}(\mathrm{Ca})\sim -5$ in the LB simulation and $\log_{10}(M)\sim 2$ and $\log_{10}(\mathrm{Ca})\sim -6$ in the experiment. The simulation and the experiment are thereby both carried out within the same dynamical region of "capillary fingering" (see Ref. [26]) and are thus comparable, although not exactly similar.

The measured and simulated saturation curves were transformed by the Washburn equation into cumulative porosities as functions of the pore-throat radius. In the simulation, radius was first calculated in lattice units and then transformed to dimensional units by simply multiplying it with the voxel size. The results are shown in Fig. 1. The two results coincide surprisingly well. We can thus assume that the simulated intrusion is a realistic representation of the experimental one.

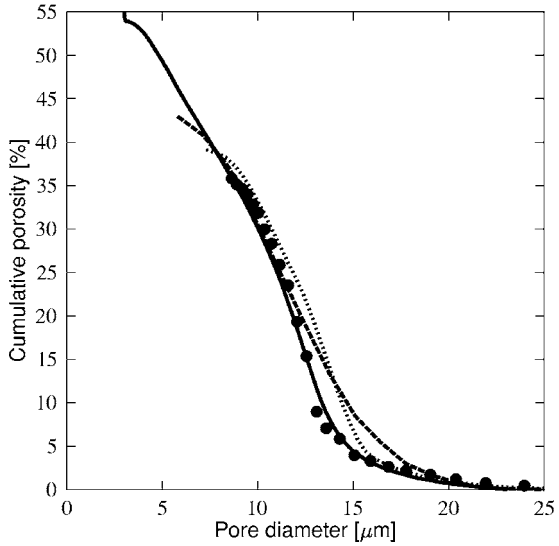

FIG. 1. Cumulative porosities as a function of pore diameter, obtained by LB simulation (solid circles), experiment (solid line), IP simulation (dotted line), and image analysis (dashed line).

Determination of pore sizes from the tomographic reconstruction was based on the algorithm of Ref. [14]. A random point in the pore space was chosen, and the pore size associated with this point was defined as the diameter of the largest sphere that fitted into the pore space and included the initial point. This procedure was then iterated sufficiently many times. A pore-throat distribution was obtained by first determining the skeleton [27] and distance map (i.e., the distances from each pore voxel to the pore walls) of the pore space. Pore throats were found as saddle points in the distance map for the skeleton. The volume attached to each pore throat was determined as the size of the pore space that could be invaded away from the closest surface such that the pore or throat diameter remained larger than or equal to that of the initial throat.

Utilizing the data obtained from these analyses we could also simulate the filling of the pore space by an IP process. In the intrusion phase the external pressure determined the minimal pore-throat size that could be invaded, while in the extrusion phase it determined the maximum size of the pores that could be evacuated. Evacuation was only possible through a continuous liquid phase reaching the sample surface. In Fig. 1, we also show the result of an IP simulation for the same sample. This simulation was affected by the discreteness of the image (pore-throat radius) more than the LB simulation, but shows, however, a qualitatively similar behavior as the LB simulation and MIP measurement. Finally, in Fig. 1, we show the pore-size distribution as obtained by image analysis. This distribution differs qualitatively from the others as it does not have a clear inflection point, thus indicating the existence of an ink-bottle effect.

Comparing the pore spaces filled at different values of pressure (pore-throat radius) by the LB and IP simulations,

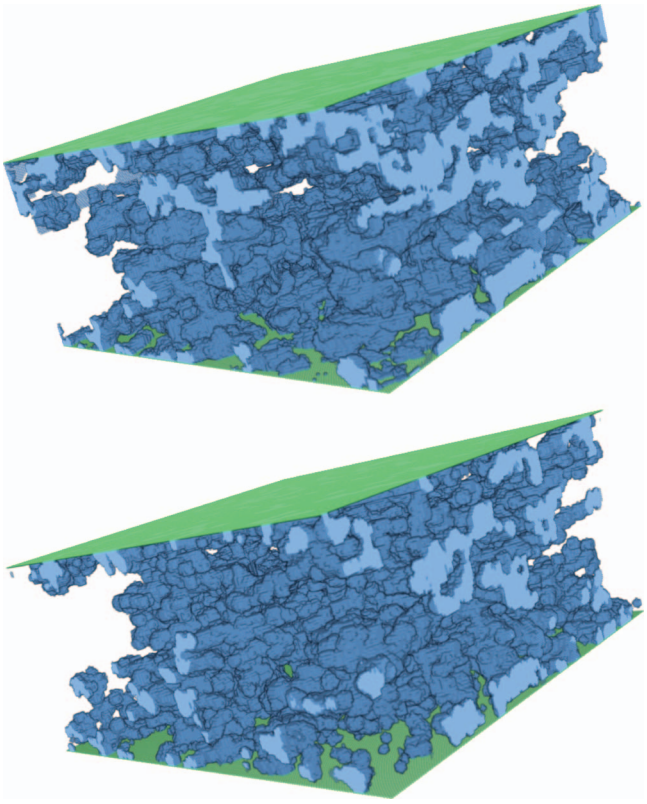

FIG. 2. (Color) Pores filled by the liquid just beyond the percolation pressure. The upper image is the LB result and the lower one the IP result.

we found that they indeed are very similar. The inflection point in the cumulative porosity gives the pressure at which the invading liquid first percolates the sample. In Fig. 2 we show the intruded liquid, just beyond the percolation pressure, as given by the two different simulations. It is evident that the intrusion process can quite well be described as one of IP.

This conclusion supports the earlier experimental observations in two dimensions (2D) of Ref. [28]. The result that the inflection point in the cumulative porosity gives the percolation pressure is also in line with earlier observations (see, e.g., Ref. [29]) and with earlier simulation results for a 2D porous-medium model [13].

To analyze the actual intrusion process in view of the common interpretation of MIP results, by which the pore space is filled in decreasing order of pore (or pore-throat) size, we determined in the LB simulation the pore-size distributions by image analysis of the filled and empty parts of the pore space at each value of pressure. A sequence of pore-size distributions for the empty part of the pore space is shown in Fig. 3. Notice that their shape remains very similar even though the pressure is increased, until the inflection point in the cumulative porosity is reached. This behavior is very different from what one expects on the basis of the common interpretation. It indicates that the ink-bottle effect is significant for paperlike porous materials and that the access function will be markedly nonlinear.

Beyond the inflection point, the pore-size distribution of the empty pore space evolves qualitatively as expected:

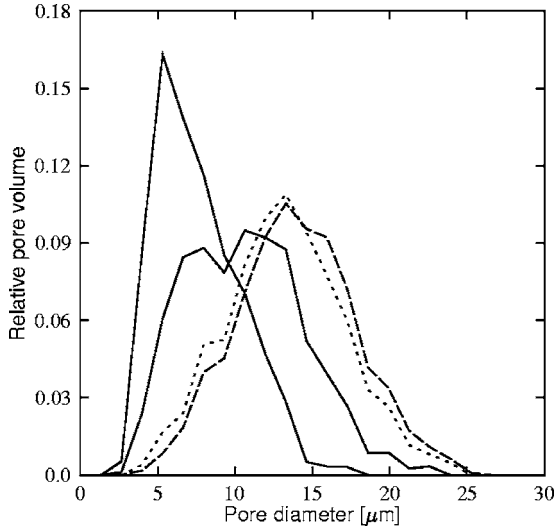

FIG. 3. Normalized pore-size distribution of the empty part of the pore space for different values of pressure. The dashed line is the distribution just before and dotted line just after the inflection point in the cumulative porosity. At low pressures the distribution does not differ much from that at the inflection point, but thereafter (solid lines) increasing pressure mostly removes the largest remaining pores that remain in the distribution.

mainly the large-size pores gradually vanish when the pressure is increased further. Notice, however, that there is no sharp cutoff in the size of the removed pores. A similar analysis of the pore-throat distributions gave exactly the same result.

The significance of the ink-bottle effect can be evaluated by determining the access function $X_a(X_{th}(p))$, where $X_{th}(p)$ is the fraction of the pore space allowed by the size of the entry pore throats at pressure p of the invading liquid [30]:

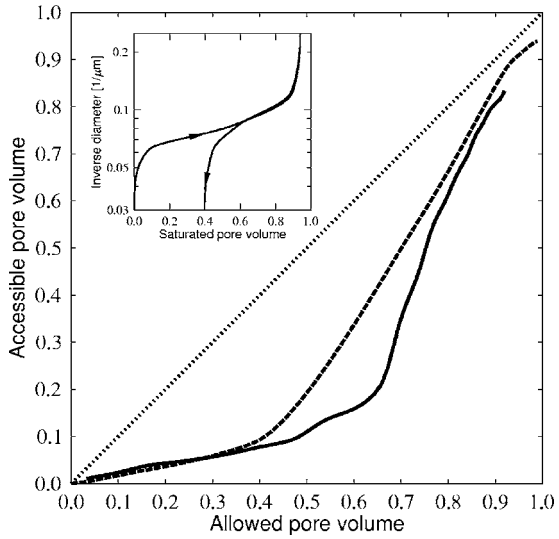

FIG. 4. The access function for the sample of paper board as determined by LB (solid line) and IP (dashed line) simulations. The dotted line is the result in the absence of the ink-bottle effect. In the inset shown are the intrusion and extrusion curve for this sample as determined by IP simulation.

$$X_{sat}(p) = X_a(X_{th}(p)). \quad (2)$$

Here $X_{sat}(p)$ is the saturation curve that we have determined experimentally by MIP, and by the LB and IP simulations (corresponding to the cumulative porosities of Fig. 1). The LB and IP access functions are shown in Fig. 4. The $X_{th}(p)$ curve was determined by image analysis from the tomographic reconstruction.

As anticipated, the access function significantly deviates from the dotted line, which would be the result from equal access to all pores—i.e., without any ink-bottle effect. Notice that the LB curve lies below the IP curve: the ink-bottle effect is somewhat underestimated by the IP analysis, which cannot completely reproduce the intrusion-extrusion process. Even then the residual saturation S_r of this process is about 0.40, which is another indication of the significance of the ink-bottle effect in paperlike materials.

For an additional check of the consistency of the IP picture, we also determined the residual saturation from the LB intrusion curve. With the usual assumptions of IP [30], the residual saturation is given by

$$S_r = S_0 - \int_{r_0}^{\infty} \frac{X_a(X_{th}(r))}{X_{th}(r)} g(r) dr, \quad (3)$$

where S_0 is the saturation at the end of intrusion, r_0 the corresponding minimum pore diameter of the filled pore space, and $g(r)$ the pore-size distribution determined from the tomographic reconstruction. If we use the LB result for the access function, we find from this equation that $S_r \approx 0.34$. This is in good agreement with the result from the IP extrusion curve.

In conclusion, we have simulated intrusion and extrusion of a nonwetting liquid in a tomographic reconstruction of a sample of paper board. The intrusion curve of the same paper board was also measured by standard MIP. When the result of the *ab initio* LB simulation was interpreted exactly as the raw data in the measurement, the resulting cumulative porosities were in excellent agreement. Comparison of the results of LB and IP simulations on the same tomographic reconstruction indicated that the intrusion process can indeed be described by invasion percolation, although agreement is not quantitatively perfect. The IP process also gave consistent results for the residual saturation of the sample after extrusion of the nonwetting liquid.

The access function, determined from the saturation curve and the pore-throat distribution for the tomographic reconstruction, indicates that the ink-bottle effect is significant in paperlike materials. The size distributions of the remaining empty pore space do not change much until the invading liquid first percolates the whole sample. It remains to be seen how important this effect is in other porous materials.

[1] C. León y León, Adv. Colloid Interface Sci. **76-77**, 341 (1998).
[2] For a review, see, e.g., M. Sahimi, Rev. Mod. Phys. **65**, 1393 (1993), and also references therein.
[3] E. W. Washburn, Proc. Natl. Acad. Sci. U.S.A. **7**, 21 (1921).
[4] H. L. Ritter and L. C. Drake, Ind. Eng. Chem. **17**, 782 (1945).
[5] H. I. Meyer, J. Appl. Phys. **24**, 510 (1953).
[6] F. A. L. Dullien and G. K. Dhawan, J. Colloid Interface Sci. **52**, 129 (1975).
[7] M. E. Fisher and J. W. Essam, J. Math. Phys. **2**, 609 (1961).
[8] P. Klobes, H. Riesemeier, K. Meyer, J. Goebbels, and K.-H. Hellmuth, Fresenius' J. Anal. Chem. **357**, 543 (1997).
[9] S. M. Sweeney and C. L. Martin, Acta Mater. **51**, 3635 (2003).
[10] S. Diamond, Cem. Concr. Res. **30**, 1517 (2000).
[11] S. Roels, J. Elsen, J. Carmeliet, and H. Hens, Mater. Struct. **34**, 76 (2000).
[12] S. Ramaswamy, S. Huang, A. Goel, A. Cooper, D. Choi, A. Bandyopadhyay, and B. V. Ramarao, in *The Science of Papermaking*, Proceedings of the 12th Fundamental Research Symposium, Pulp and Paper Fundamental Research Society, Oxford, UK, 2001, edited by C. F. Baker (Pulp and Paper Fundamental Research Society, Bury, Lancashire, UK, 2001), pp. 1289–1311.
[13] E. J. Garboczi and D. J. Bentz, Ceram. Trans. **16**, 265 (1991).
[14] J. F. Delerue, E. Perrier, Z. Y. Yu, and B. Velde, Phys. Chem. Earth, Part A Solid Earth Geod. **24**, 639 (1999).
[15] For the typical structure of paperlike materials, see, e.g., M. Alava and K. Niskanen, Rep. Prog. Phys. **69**, 669 (2006).
[16] S. Succi, *The Lattice Boltzmann Equation for Fluid Dynamics and Beyond* (Oxford University Press, Oxford, 2001).
[17] S. Chen and G. D. Doolen, Annu. Rev. Fluid Mech. **30**, 329 (1998).
[18] X. Shan and H. Chen, Phys. Rev. E **47**, 1815 (1993); **49**, 2941 (1994).
[19] J. Hyväluoma, P. Raiskinmäki, A. Jäsberg, A. Koponen, M. Kataja, and J. Timonen, FGCS, Future Gener. Comput. Syst. **20**, 1003 (2004).
[20] F. M. van Kats and P. J. P. Egberts, Transp. Porous Media **37**, 55 (1999).
[21] C. Pan, M. Hilpert, and C. T. Miller, Water Resour. Res. **40**, W01501 (2004).
[22] M. C. Sukop and D. Or, Water Resour. Res. **40**, W01509 (2004).
[23] H.-J. Vogel, J. Tölke, V. P. Schulz, M. Krafczyk, and K. Roth, Vadose Zone J. **4**, 380 (2005).
[24] A. Valfouskaya and P. M. Adler, Phys. Rev. E **72**, 056317 (2005).
[25] J. Hyväluoma, P. Raiskinmäki, A. Jäsberg, A. Koponen, M. Kataja, and J. Timonen, Phys. Rev. E **73**, 036705 (2006).
[26] R. Lenormand, E. Touboul, and C. Zarcone, J. Fluid Mech. **189**, 165 (1988).
[27] K. Palgyi and A. Kuba, Pattern Recogn. Lett. **19**, 613 (1998).
[28] J.-D. Chen and J. Koplik, J. Colloid Interface Sci. **108**, 304 (1985).
[29] A. J. Katz and A. H. Thompson, Phys. Rev. B **34**, 8179 (1986).
[30] R. G. Larson and N. R. Morrow, Powder Technol. **30**, 123 (1981).